

## Spin-glass transition of a dilute Ag-Mn alloy in a magnetic field

M. A. Novak,\* O. G. Symko, and D. J. Zheng†

*Department of Physics, University of Utah, Salt Lake City, Utah 84112*

(Received 26 August 1985)

The spin-glass state in a magnetic field is studied in a very dilute Ag-Mn sample containing 150 ppm of Mn. The field-cooled magnetization of this system is investigated over temperatures ranging from 4 down to 0.01 K in magnetic fields from 932 to 1 Oe. Scaling is observed in the nonlinear susceptibility above  $T_g$  and in the order parameter below  $T_g$ . The critical exponents are in good agreement with those obtained on much-higher-concentration spin glasses and are different from the mean-field values. There is strong evidence for a phase transition.

## I. INTRODUCTION

The spin-glass state has been investigated with a variety of experimental and theoretical techniques, the central question being whether there exists a true thermodynamic phase transition at the spin freezing temperature  $T_g$ . In the past few years there has been increasing evidence pointing toward the existence of a phase transition. Susceptibility data<sup>1</sup> on concentrated spin glasses have been explained in terms of a non-mean-field scaling theory.<sup>2</sup> Recent EPR linewidth studies<sup>3,4</sup> did show that near  $T_g$  for  $T > T_g$ , scaling behavior was observed for the critical part of the linewidth. Theoretically, the scaling laws as applied to spin glasses have been extensively discussed.<sup>5,6</sup>

We present here a study of the magnetization of a very dilute spin glass, Ag-Mn, whose  $T_g$  is 0.15 K. Such a low  $T_g$  gives an easy access to a wide range of magnetic fields for investigating the behavior of the spin-glass transition and state in a magnetic field. In fact, in this work we scan the magnetic field up to a field parameter  $h = 0.8357$ , where  $h$  is equal to  $g\mu_B H / k_B T_g$  and  $H$  is the applied magnetic field. The original Edwards-Anderson model<sup>7</sup> shows that there is no transition in a magnetic field because the order parameter is then always nonzero. However, experimental<sup>8</sup> and theoretical<sup>9</sup> work based on the Sherrington-Kirkpatrick model<sup>10</sup> shows a phase transition in a magnetic field. Our investigation of such a very dilute system will provide general characteristics of a spin-glass system which can be compared to the very-high-concentration spin glasses studied so extensively. In this work we study the spin-glass transition above and below  $T_g$ , the sample being field cooled. There is general belief that field cooling of the sample yields a thermodynamic equilibrium state or quasiequilibrium state.<sup>10</sup>

The authors of Ref. 11 have studied the entire  $H$ - $T$  phase diagram, arguing that, at fixed field, on reducing the temperature the system first undergoes a crossover at temperatures  $T_x(H)$  from paramagnetic behavior to a region of nonlinear susceptibility. Only at the lowest temperatures, at and below  $T_g(H)$ , where  $T_g(H) < T_g(0)$ , the system enters the spin-glass state. According to mean-field theory, the transition temperature  $T_g(H)$  follows a  $\frac{2}{3}$  power law, which is more or less close to experimental results, but the prediction of  $T_x(H)$  is far away from experi-

mental results. The non-mean-field scaling theory proposed by Malozemoff *et al.*<sup>1,2</sup> gives a reasonable explanation for  $T_g(H)$  and  $T_x(H)$  for the spin glasses Gd-Al and Cu-Mn.

The present paper presents experimental details of the measurements, followed by an analysis of the spin-glass state above and below  $T_g$ . Because of the nature of the measurements at very low temperatures, each point corresponds to an equilibrium point, the waiting time for each point being 2–3 h. Our results do not deal with irreversibilities and hence we present a new approach in analyzing the equilibrium data in the spin-glass state.

## II. EXPERIMENTAL DETAILS

The magnetization of the sample was measured with a SQUID (superconducting quantum-interference device) magnetometer, the external field  $H$  being trapped in a superconducting niobium cylinder surrounding the sample. The Mn spin contribution is obtained by subtracting the background signal from a piece of pure Ag used in the fabrication of the Ag-Mn alloy. Such subtraction is possible by using an astatic pair of coils coupling the flux from the samples to the SQUID magnetometer.<sup>12</sup> Cooling is produced by a <sup>3</sup>He-<sup>4</sup>He dilution refrigerator, and the sample is located inside the mixing chamber, in good contact with the dilute phase of the mixture. Temperatures were measured by a cerium magnesium nitrate magnetic thermometer coupled to another SQUID magnetometer. The samples were field cooled over a period of hours, and data were taken on warming of the sample in small temperature increments and after equilibrium had been established between the thermometer and the sample.

The sample consisted of polycrystalline Ag-Mn alloy formed from 6N pure Ag and 4N Mn in an induction furnace; it was machined to a cylinder 6.25 mm long and 2.5 mm in diameter. During the preparation of the sample the alloy was well mixed by the induced currents for several minutes and then dropped into a room-temperature mold in order to facilitate a rapid quench from the melt. The concentration was determined by atomic absorption analysis.

### III. ANALYSIS OF DATA

The data that were obtained are shown in Fig. 1. The figure shows the magnetization normalized to the magnetic field  $H$  as a function of temperature for a wide range of external magnetic fields ranging from 1 to 932 Oe. This graph shows the change from the paramagnetic state to the spin-glass state, the sharpness of this change depending on the magnetic field. In our analysis we start with an approach proposed by Malozemoff *et al.*,<sup>1</sup> but then, when in the spin-glass state, we present a new approach in dealing with this state, which is based on the characteristics of the order parameter and its scaling behavior. Hence, we divide the analysis for the temperature regimes  $T > T_g$ ,  $T_g$ ,  $T < T_g$ , and then the combined behavior is used to construct a phase diagram  $(H, T)$ .

#### A. Determination of $T_g$ .

The strongest critical behavior occurs not in the linear susceptibility  $\chi_0$  but in the nonlinear susceptibility  $\chi_0 - \chi$ . Since we are measuring the magnetization  $M(T)$ , a field expansion of the normalized magnetization gives

$$M(T)/H = \chi_0(T) - \chi_2(T)H^{\alpha(T)}, \quad (1)$$

where  $\chi_2(T)$  is the nonlinear susceptibility. The linear susceptibility  $\chi_0(T)$  is determined by a linear extrapolation to zero field of the  $M(T)$  results in fields of 10–1 Oe. A log-log plot of  $\chi_0 - M/H$  against  $H$  is used to determine  $\chi_2(T)$  and  $\alpha(T)$  for each temperature. From such an analysis the quantities  $\chi_0$ ,  $\chi_2$ , and  $\alpha$  are extracted; Fig. 2 shows the temperature dependence of these quantities. The linear susceptibility is approximately temperature independent for  $T < T_g$ ; the nonlinear susceptibility  $\chi_2$  has a maximum at the transition temperature  $T_g$ , while the exponent  $\alpha(T)$  has a minimum at that temperature. From the maximum in  $\chi_2$ , for this spin glass of Ag-Mn (150 ppm Mn), we determine that  $T_g = 0.15$  K in the zero-field limit.

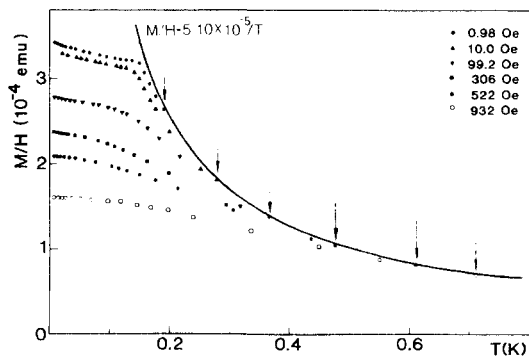


FIG. 1. Magnetization normalized to magnetic field as a function of temperature for 150 ppm Ag-Mn. Solid line shows paramagnetic behavior and arrows indicate temperatures at which departures from Curie's law occur.

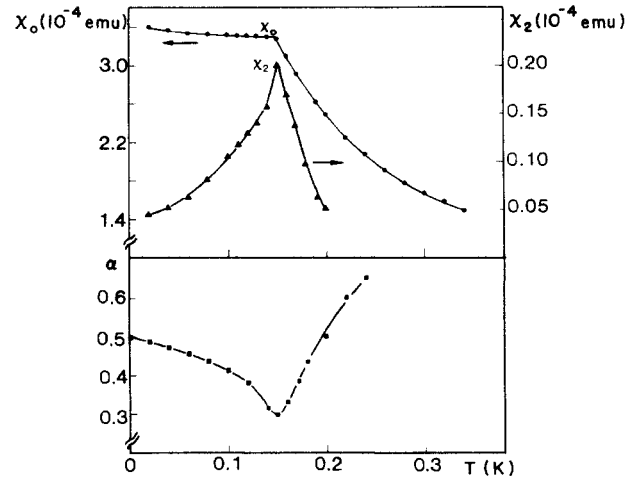


FIG. 2. Temperature dependence of linear susceptibility  $\chi_0$ , nonlinear susceptibility  $\chi_2$ , and exponent  $\alpha$ .

#### B. Scaling at $T > T_g$

Having extracted the nonlinear susceptibility from the data, we analyze it in terms of a non-mean-field scaling theory where

$$\chi_2 = \chi_0(T) - M(T)/H = H^{2/\delta} f(t/H^{2/\phi}), \quad (2)$$

where

$$f(x) \begin{cases} \rightarrow \text{const} & \text{as } x \rightarrow 0, \\ \sim x^{-\gamma} & \text{as } x \rightarrow \infty, \end{cases}$$

and  $\delta, \gamma, \phi$  are critical exponents. Here  $t$  is the reduced temperature  $(T - T_g)/T_g$ . In order for the behavior to be regular above  $T_g$ , the exponents must satisfy the scaling relation

$$\phi = \delta\gamma / (\delta - 1). \quad (3)$$

The nonlinear susceptibility  $\chi_2$  is fitted to Eq. (2) by plotting  $[\chi_2(t)/H^{2/\delta}]$  versus  $(t/H^{2/\phi})$  on double-logarithmic scales for different values of the pair of exponents  $(\phi, \delta)$ . The best scaling is obtained for  $\delta = 6.6$  and  $\phi = 4.5$ , and this is shown in Fig. 3(a). Now, the nonlinear susceptibility exponent  $\gamma$  is calculated from Eq. (3) to be 3.8. Such a large exponent value implies a rapid thermal variation of  $\chi_2$  since  $\chi_2$  varies as  $H^2 t^{-\gamma}$ . The good fit of the nonlinear susceptibility to Eq. (2) implies that it diverges as  $t^{-\gamma}$  as  $T_g$  is approached from the high-temperature side and that it goes as  $H^{2/\delta}$  at  $T_g$ . The exponents that we obtained differ from those of a mean-field model, where  $\gamma = 1$ ,  $\phi = 2$ , and  $\delta = 2$ ; however, they are in good agreement with the values obtained, for example, by Malozemoff *et al.*<sup>1</sup> for Gd-Al and Cu-Mn spin glasses. Their values for Gd-Al are  $\gamma = 3.8$ ,  $\delta = 5.7$ , and  $\phi = 4.5$ .

#### C. Scaling at $T < T_g$

This is the regime where the system is in the spin-glass phase. Because the measurements are taken in a wide

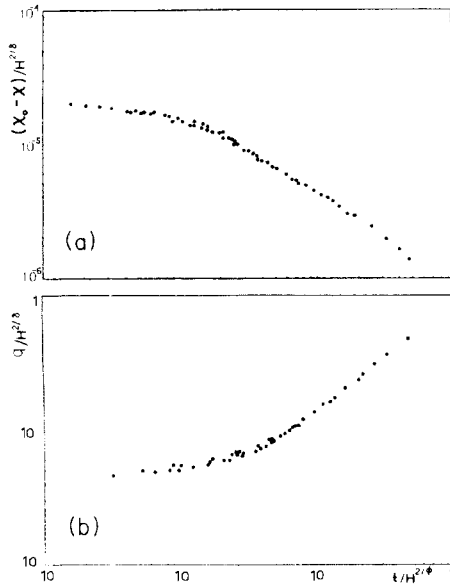


FIG. 3. Scaling behavior of Ag-Mn. (a) Scaling of nonlinear susceptibility  $\chi_2$  at  $T > T_g$ . (b) Scaling of order parameter  $q$  at  $T < T_g$ .

range of magnetic fields, the spin-glass state will occur at temperature  $T_g(H)$  or below, where  $T_g(H) < T_g(0)$ . Generally, the transition temperature  $T_g(H)$  in finite fields is defined as the onset of irreversible magnetization. However, our magnetization measurements are field-cooled dc measurements, and therefore they are true thermodynamic values or close to it; the field is not changed. Hence, we determine  $T_g(H)$  from the behavior of the order parameter  $q$  rather than the onset of irreversibilities since we do not measure them.

According to Fischer's<sup>13</sup> formula relating the order parameter  $q$  to the susceptibility,

$$q = 1 - \frac{T\chi}{c}, \quad (4)$$

where  $c$  is Curie's constant and the Curie-Weiss temperature is zero. If  $\chi$  is independent of temperature,  $q$  should have a linear variation with temperature. Hence, a set of curves of  $q$  as determined from Eq. (4) varying with temperature is plotted for the various applied magnetic fields. The deviation of  $q$  from a straight line is used as the criterion to determine the transition temperature  $T_g(H)$  for each field. The higher the field, the lower the transition temperature  $T_g(H)$  for the spin-glass state. These measurements will be discussed in the next section.

Since we have used the order parameter  $q$  to determine  $T_g(H)$ , we raised the question as to whether the order parameter can also follow a scaling function such as

$$q(H, t) = H^{2/\delta'} f(t/H^{2/\phi}), \quad (5)$$

where, as before,

$$f(x) \begin{cases} \rightarrow \text{const} & \text{as } x \rightarrow 0, \\ \sim x^\beta & \text{as } x \rightarrow \infty, \end{cases} \quad (6)$$

and  $\phi = \beta\delta'$ .

We have plotted  $[q(H, t)/H^{2/\delta'}]$  versus  $(t/H^{2/\phi})$  on double-logarithmic scales for various values of  $(\phi, \delta')$ . Here  $t$  is  $(T_g - T)/T_g$  since we are below  $T_g$ . Scaling occurs for  $\delta' = 5.4$  and  $\phi = 4.5$ , and this scaling of the experimental results is shown in Fig. 3(b). We measure  $\delta'$  different from  $\delta$ , although they are almost the same; the exponent  $\phi$  is the same below and above  $T_g$ . The exponent of the order parameter is then given by Eq. (6) and it is  $\beta = 0.83$ .

#### D. Phase diagram $(H, T)$

From all the information obtained in the above analysis, it is possible now to construct a phase diagram  $(H, T)$ . The system starts at high temperatures in the paramagnetic regime; as the temperature is reduced it goes into a regime where the nonlinear behavior of the susceptibility dominates (presumably due to the formation of various clusters), and finally at lower temperatures the system goes into the spin-glass state. The spin-glass state is separated from the nonlinear regime by a line of temperatures  $t_g(H)$ , while the nonlinear part is separated from the paramagnetic regime by the temperatures  $t_x(H)$ . From our analysis these regimes are separated by  $t_g(H) = 0.04H^{2/\phi}$  and  $t_x(H) = 1.8H^{2/\phi}$ , and this is shown in Fig. 4. Such a phase diagram is different from the usual representation,<sup>1</sup> where irreversibilities play an important role below  $t_x(H)$ . However, magnetocaloric measurements by Berton *et al.*<sup>14</sup> on a more concentrated spin glass also show a similar equilibrium phase diagram, not dealing with irreversibilities.

#### IV. DISCUSSION

The measurements presented here on a very dilute spin glass at concentration levels of 150 ppm show behavior very similar to other spin glasses whose impurity concentrations are larger by many orders of magnitude (for example, Gd-Al in Ref. 1 has 37 at. % of Gd). The fact that the spin-glass transition  $T_g$  is so low for our sample makes it easier to span a large range of magnetic fields. Our results span a very large field range,  $h$  being 0.8357,

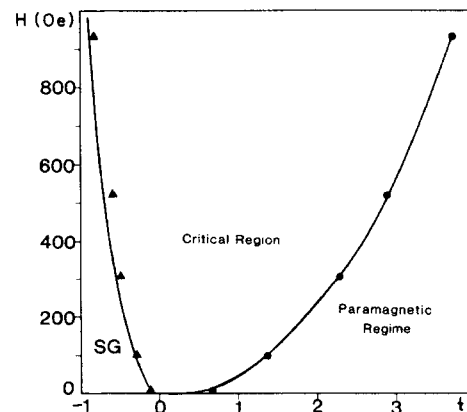


FIG. 4. Phase diagram  $(H, t)$  of 150 ppm Ag-Mn spin glass.

in contrast with an  $h$  of 0.008 in Ref. 8 and 0.06 in Ref. 1. We observe scaling behavior above and below  $T_g$ . Also, in contrast to most other measurements, we have investigated only the field-cooled, thermodynamic equilibrium state of the spin glass with no field cycling. Based on the assumption that we have an equilibrium state which has experimental support,<sup>15</sup> our magnetization does not change with time. We have investigated the behavior of the order parameter in the spin-glass state. To analyze our data we needed only one order parameter. As mentioned earlier, our  $(H, T)$  phase diagram has a different interpretation from the usual one in that it deals with equilibrium behavior. In that respect it is similar to that of Ref. 14. Although attempts have been made in trying to identify the de Almeida–Thouless<sup>9</sup> and Sompolinsky<sup>16</sup> longitudinal instability line  $t_g(H) = -AH^{2/3}$  and the Gabay–Toulouse transverse freezing line<sup>17</sup> with experimental results at low  $h$ , our results do not agree with such mean-field behavior; our  $t_g(H)$  line depends on  $H^{2/\phi}$  with

$\phi=4.5$  for a large range of  $h$ . The significance of the phase diagram in Fig. 4 is that below  $t_g(H)$  the system enters the spin-glass phase, above  $t_x(H)$  it is in the paramagnetic phase, and in between it has strong non-linear behavior dominated by the magnetic field. It is remarkable that our very-low-concentration spin glass gives results which are comparable to concentrated spin glasses (for example, results of Ref. 3 give  $\phi=5.0$ ). The evidence presented in this paper, which complements previous work in this area, suggests that there is a true thermodynamic phase transition at  $T_g$ .

#### ACKNOWLEDGMENTS

We acknowledge interesting and informative discussions with Professor D. Mattis. This work was supported in part by the National Science Foundation. One of us (M.A.N.) acknowledges financial assistance from Conselho Nacional de Desenvolvimento Científico e Tecnológico (CNPq), Brazil.

\*Present address: Universidade Federal do Rio de Janeiro, Instituto de Física, Ilha de Fundão, Rio de Janeiro, Brazil.

†On leave from the Chinese Academy of Sciences, Beijing, People's Republic of China.

<sup>1</sup>A. P. Malozemoff, B. Barbara, and Y. Imry, *J. Appl. Phys.* **53**, 2205 (1982); **53**, 7672 (1982).

<sup>2</sup>S. E. Barnes, A. P. Malozemoff, and B. Barbara, *Phys. Rev. B* **30**, 2765 (1984).

<sup>3</sup>W. Wu, G. Mozurkewich, and R. Orbach, *Phys. Rev. B* **31**, 4557 (1985).

<sup>4</sup>D. L. Huber, *Phys. Rev. B* **31**, 4420 (1985).

<sup>5</sup>B. Barbara, A. P. Malozemoff, and S. E. Barnes, *J. Appl. Phys.* **55**, 1655 (1984).

<sup>6</sup>D. S. Fisher and H. Sompolinsky, *Phys. Rev. Lett.* **54**, 1063 (1985).

<sup>7</sup>S. F. Edwards and P. W. Anderson, *J. Phys. F* **5**, 965 (1975).

<sup>8</sup>R. V. Chamberlin, M. Hardiman, L. A. Turkevich, and R. Or-

bach, *Phys. Rev. B* **25**, 6720 (1982).

<sup>9</sup>J. R. L. de Almeida and D. J. Thouless, *J. Phys. A* **11**, 983 (1978).

<sup>10</sup>D. Sherrington and S. Kirkpatrick, *Phys. Rev. Lett.* **35**, 1792 (1975).

<sup>11</sup>J. Vannimenus, G. Toulouse, and G. Parisi, *J. Phys. (Paris)* **42**, 201 (1981).

<sup>12</sup>T. J. Steelhammer and O. G. Symko, *Rev. Sci. Instrum.* **50**, 532 (1979).

<sup>13</sup>K. H. Fischer, *Phys. Rev. Lett.* **34**, 1438 (1975).

<sup>14</sup>A. Berton, J. Chaussy, J. Odin, R. Rammel, and R. Tournier, *J. Phys. (Paris) Lett.* **43**, L153 (1982).

<sup>15</sup>W. E. Fogle, J. D. Boyer, R. A. Fisher, and N. E. Phillips, *Phys. Rev. Lett.* **50**, 1815 (1983).

<sup>16</sup>H. Sompolinski, *Phys. Rev. Lett.* **47**, 935 (1981).

<sup>17</sup>M. Gabay and G. Toulouse, *Phys. Rev. Lett.* **47**, 201 (1981).